Title: Genotyping of common *EGFR* mutations in lung cancer patients by electrochemical biosensor

Authors: Xiu-Hua Weng, Xiong-Wei Xu, Chang-Lian Wang, Wei-Wei Lin, Ai-Lin Liu, Wei Chen, Xin-Hua Lin

PII: S0731-7085(17)32716-4
DOI: https://doi.org/10.1016/j.jpba.2017.12.015
Reference: PBA 11668

To appear in: *Journal of Pharmaceutical and Biomedical Analysis*

Received date: 1-11-2017
Revised date: 6-12-2017
Accepted date: 7-12-2017

Please cite this article as: Xiu-Hua Weng, Xiong-Wei Xu, Chang-Lian Wang, Wei-Wei Lin, Ai-Lin Liu, Wei Chen, Xin-Hua Lin, Genotyping of common EGFR mutations in lung cancer patients by electrochemical biosensor, Journal of Pharmaceutical and Biomedical Analysis https://doi.org/10.1016/j.jpba.2017.12.015

Genotyping of common *EGFR* mutations in lung cancer patients by electrochemical biosensor

Xiu-Hua Weng,[a] Xiong-Wei Xu,[a,*] Chang-Lian Wang,[a] Wei-Wei Lin,[a] Ai-Lin Liu,[b] Wei Chen,[b,*] Xin-Hua Lin[b,*]

[a] Department of Pharmacy, First Affiliated Hospital of Fujian Medical University, Fuzhou, Fujian 350005, PR China

[b] Department of Pharmaceutical Analysis, Fujian Medical University, Fuzhou, Fujian 350004, PR China

[*]Corresponding author. Tel: +86 591 87981630, fax: +86 591 87981331. E-mail address: xxw0409@sina.com, chenandhu@163.com, xhl1963@sina.com

Graphical abstract

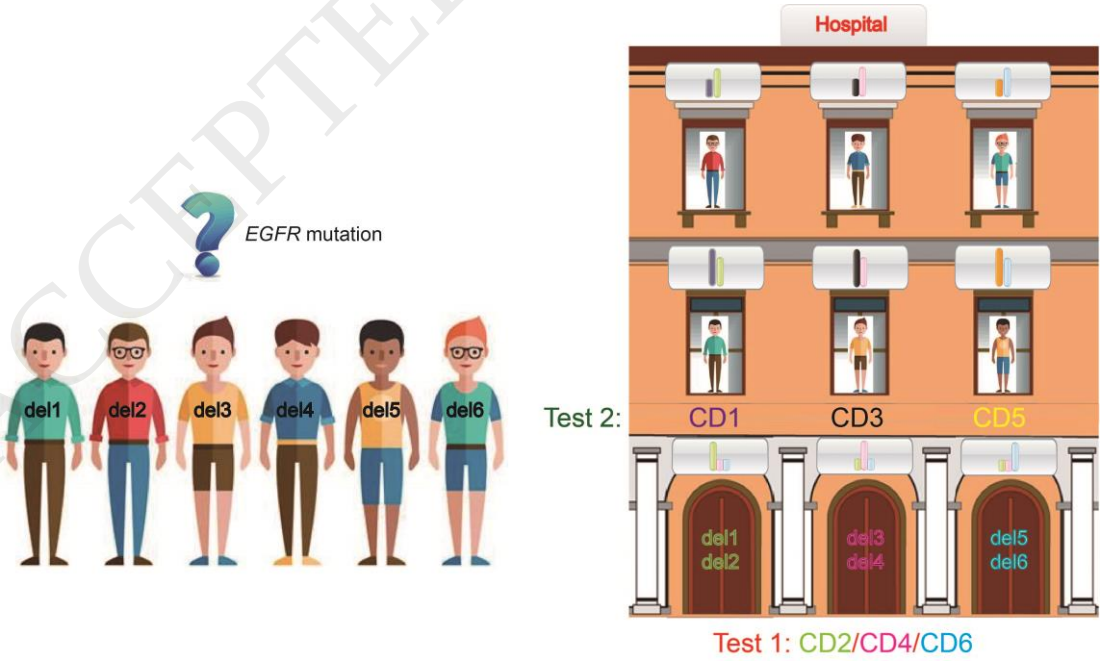

A grouped detection method was developed to reduce the workload and allow quick identification of any of the six common EGFR exon 19 deletion types. Sequencely, EGFR exon 19 mutation types of lung cancer patients were indentified successfully after PCR amplification and Lambda exonuclease (λ-exo) assisted ssDNA generation.

Highlights

- ● Electrochemical biosensor for genotyping of common *EGFR* mutations.
- ● Influence of non-complementary location on discrimination ability.
- ● Capture probe with non-complementary location in its middle part has the highest hybridization specificity
- ● A grouping approach realizes faster identification of specific mutations.
- ● Genotyping of common *EGFR* mutations for lung cancer patients.

Abstract

In this study, we constructed a sandwich-type biosensor to identify six common types of mutations in exon 19 of the epidermal growth factor receptor (*EGFR*) gene, and tested them using tissue samples from patients with non-small cell lung carcinomas. Considering the characteristics that different locations of non-complementary in DNA probes resulting in different hybridization efficiency, we investigated the design of DNA capture probes with varying non-complementary sequence locations in an effort to optimize the selectivity of the biosensor. Our results revealed that non-complementary sequences located in the middle of a capture probe allow excellent hybridization specificity and achieve the strongest discrimination between mutations that differ by a single nucleotide. Based on this finding, we designed capture probes to identify six common types of *EGFR* mutations (del1-del6)

successfully. Further, we proposed a grouped testing approach to reduce workload and rapidly identify mutation types. Subsequently, *EGFR* exon 19 hotspot deletion types in real samples were discriminated by this method. RT-PCR products from lung cancer patients were digested with λ-Exo and analyzed using electrochemical biosensors. The results of our grouped testing approach with optimized biosensors were consistent with that of direct sequencing, suggesting that our proposed protocol can be excellent candidate for genotyping of *EGFR* mutations in lung cancer patients.

Keywords: electrochemical biosensors; genotyping; epidermal growth factor receptor; mutation; non-small cell lung carcinoma; grouped testing approach

1. Introduction

Mutation of the epidermal growth factor receptor gene (*EGFR*) is an important predictor of tumor response to small molecule tyrosine kinase inhibitors (TKIs), which exert efficient effect for *EGFR* mutation-positive lung cancer. *EGFR* mutations are found in 10-40% of non-small cell lung cancer (NSCLC) patients [1]. Exon 19 of *EGFR* encodes part of its tyrosine kinase domain. Mutations of exon 19 facilitate the binding of TKIs within the ATP binding pockets in the tyrosine kinase domain of EGFR, thus preventing EGFR from binding ATP. Consequently, downstream signaling is blocked, cellular proliferation and differentiation are inhibited, and apoptosis is induced [2]. There are six common types of hotspot mutations in *EGFR* exon 19, which are mostly located in the sequence encoding the 746th to the 753rd amino acids, and are primarily deletions affecting the β3 strand or the αC helix [3-6].

The sensitivity of EGFR to TKIs depends on specific mutations [7, 8]. Therefore, it is important to distinguish mutation genotypes of *EGFR* exon 19 in the clinical setting, to inform treatment and improve patient prognoses.

In recent years, an impressive number of electrochemical DNA sensors have been developed and employed to detect specific nucleotide sequences [9-24]. Among them, the sandwich-type strategy, which involved a pair of DNA probes (capture and reporter probes) that flanked the target DNA sequence, processes significantly improved signal-to-noise ratio, thus enabling the reliable detection of as low as picomolar DNA targets [25]. The high sensitivity of electrochemical transducers, as well as their compatibility with modern microfabrication and miniaturization technologies makes such devices promising solution for the point-of-care diagnostics. The key to identifying common mutations in DNA is to improve the detection specificity of DNA biosensors. DNA hybridization efficiency is inversely correlated with specificity, as confirmed by our preliminary studies [26]. A more favorable environment for hybridization leads to higher hybridization efficiency, but results in reduced hybridization specificity. Inevitably, a sandwich-type DNA biosensor based on high-efficiency DNA hybridization would have a lower specificity. Studies have shown that for regular liquid-phase DNA hybridization, the location of non-complementary sequences within the DNA affects hybridization efficiency due to differences in the continuity and stability of the formed double-stranded DNA (dsDNA) [27-30]. Gotoh *et al.* stated that for a DNA probe fixed to a solid surface, changing the location of a fixed number of mismatched bases can cause up to a

seven-fold change in the hybridization equilibrium association constant (Ka) [29]. For sandwich-type electrochemical biosensors which undergo heterogeneous hybridization on electrode surfaces, there are no relevant studies on the influence of the non-complementary sequence location on the hybridization efficiency and biosensor specificity.

Our preliminary studies have confirmed that sandwich-type DNA electrochemical biosensors can effectively distinguish wild-type *EGFR* from *EGFR* containing deletions [26]. In addition, the hybridization between non-complementary sequences taken place in a heterogeneous environment on electrode surface results in low hybridization efficiency and high biosensor specificity. Based on our preliminary findings, this study aimed to improve the identification of six common *EGFR* exon 19 deletions and to achieve rapid discrimination between them using sandwich-type DNA electrochemical biosensors. In order to optimize probe specificity, we first used two deletions (del1, del2) that had only one base difference to investigate the influence of non-complementary sequence location within a probe. Next, we attempted to expand the use of the approach we established to differentiate between other deletion types. Importantly, we developed a grouped detection method that reduced the workload and allowed quick identification of any of the six common *EGFR* exon 19 deletion types. Finally, we demonstrated the application of our grouped detection method by successfully identifying *EGFR* exon 19 mutations in tissue samples from lung cancer patients.

2. Material and methods

2.1. Reagents

The 3,3',5,5'-tetramethylbenzidine (TMB) substrate (Neogen K-blue low-activity substrate) was from Neogen (Lansing, USA). Avidin-horseradish peroxidase (HRP) was from Roche Diagnostics. Bovine serum albumin was obtained from Roche Diagnostics (Mannheim, Germany) and used without further purification. λ-Exo was from New England Biolabs (Ipswich, USA). The buffer solutions used in this study were as follows: The DNA immobilization buffer contained 10 mM Tris-HCl, 1 mM ethylenediaminetetraacetic acid, and 1 M NaCl (pH 8.0). The hybridization buffer was a 10 mM phosphate buffer (PB) solution containing 1 M NaCl (pH 7.4). λ-Exo reaction buffer contained 67 mM Glycine-KOH, 2.5 mM $MgCl_2$, and 50 μg/ml BSA (pH 9.4). All solutions were prepared with Milli-Q water (18 MΩ cm resistivity) from a Millipore system.

2.2. Nucleotide sequences

Human *EGFR* mRNA sequence information was extracted from the NCBI GenBank database (http://www.ncbi.nlm.nih.gov/genbank/, accession number Ay588246). Six sequences (del1-del6) were designed to correspond to the most prevalent mutations of exon 19 reported in the literatures [3-6]. All oligonucleotides were synthesized and purified by TaKaRa Inc. (Dalian, China), and the sequences are listed as follows:

Capture probe:

CapA: 5'-SH-tttt-ttccttgttggctttcggagatgtc-3'

CapB: 5’-SH-tttt-tcggagatgtcttgatagcgacggg-3’

CapC: 5’-SH-tttt-cttgatagcgacgggaattttaact-3’

Cd1: 5’-SH-tttt-tcggagatgttttgatagcgacggg-3’

Cd2: 5’-SH-tttt-tcggagatgtcttgatagcgacggg-3’

Cd3: 5’-SH-tttt-atgttggttccttgatagcgacggg-3’

Cd4: 5’-SH-tttt-gagatggttccttgatagcgacggg-3’

Cd5: 5’-SH-tttt-ctttcggttccttgatagcgacggg-3’

Cd6: 5’-SH-tttt-ctttcggaaccttgatagcgacggg-3’

Reporter probe:

5’-ttctcaccttctgggatccagagtc-3’

Target:

del1:

5’-gactctggatcccagaaggtgagaaagttaaaattcccgtcgctatcaaaacatctccgaaagccaacaaggaa-3’

del2:

5’-gactctggatcccagaaggtgagaaagttaaaattcccgtcgctatcaagacatctccgaaagccaacaaggaa-3’

del3:

5’-gactctggatcccagaaggtgagaaagttaaaattcccgtcgctatcaaggaaccaacatctccgaaagccaacaag
gaa-3’

del4:

5’-gactctggatcccagaaggtgagaaagttaaaattcccgtcgctatcaaggaaccatctccgaaagccaacaagga
a-3’

del5:

5’-gactctggatcccagaaggtgagaaagttaaaattcccgtcgctatcaaggaaccgaaagccaacaaggaa-3’

del6:

5’-gactctggatcccagaaggtgagaaagttaaaattcccgtcgctatcaaggttccgaaagccaacaaggaa-3’

2.3. Electrochemical biosensor preparation

A CHI660D electrochemical analyzer (Shanghai, China) was used to perform the amperometric experiments, which was connected to a conventional Au disk working electrode (2 mm diameter), an Ag/AgCl reference electrode, and a Pt wire auxiliary electrode. The BSA-based biosensor was fabricated according to a protocol developed previously [31]. Briefly, the polished Au electrode was incubated with 0.1% BSA for 15 min at room temperature. A 3 μL volume of 1 μM capture probe DNA solution was dropped on the BSA-modified gold electrode and incubated for 1 h at room temperature. Finally, the electrode was thoroughly rinsed with water and dried under nitrogen.

2.4. DNA hybridization detection

The DNA detection protocol involved a sandwich-type hybridization assay and the capture of the HRP enzyme tag. Different concentrations of the DNA target were mixed with the biotinylated reporter probe (20 nM) in the hybridization buffer. Then the mixture was incubated with capture probe which had been immobilized on electrode surface. A 3 μL volume of avidin-HRP (0.5 U/mL) was dropped on the electrode surface and incubated for 15 min at room temperature. Finally, the electrode was extensively rinsed and subjected to electrochemical measurements. Amperometric detection was performed in TMB substrate, and the current was

sampled at 100 s. Each experiment was repeated at least three times.

2.5. PCR amplification of *EGFR* from real samples

The real samples came from lung cancer patients who accepted neoplasms resection operation. All patients were from the Chest Surgery Department of First Affiliated Hospital of Fujian Medical University (Fujian, China). Genomic DNA was extracted from liquid-nitrogen-frozen tumor tissue of patients by using Trizol as per manufacturer's instructions (Invitrogen) and DNA was quantified by UV-visible spectrophotometry at 260 nm (SpectrumLab 752S, China). PCR amplification reaction was set up in 50 μL volume consisting of 5.0 μL 10X buffer (10 mM Tris-HCl, 50 mM KCl, and 1.5 mM $MgCl_2$), 0.2 mM dNTPs, 20 pmol of each primer, 1 μg genomic DNA, and 1.5 μL Taq (Takara, Japan). Amplification was performed on a thermal cycler instrument (MyGenie32, Bioneer, Korea). The reaction comprised initial denaturation at 94 °C for 5 min, followed by 35 cycles of denaturation 94 °C for 30 s, annealing at 57 °C for 30 s, and extension at 72 °C for 30 s. Final extension was carried out at 72 °C for 5 min. The PCR products were diluted and then their optical densities (OD) at 260 nm and 280 nm wavelengths were measured using a UV spectrophotometer. The PCR product concentrations were calculated using the Beer-Lambert law ($A = \varepsilon \cdot b \cdot c$). Aliquots of 5 μL of the PCR products were electrophoresed on 1.5 % agarose gels containing EB for 1-1.5 h. The GeneRuler 100 bp DNA ladder (Fermentas) was used as a marker. The gels were then visualized under an ultraviolet transilluminator and photographed. At the same time, the PCR amplification products were detected by the proposed electrochemical biosensor.

2.6. ssDNA preparation

The λ-Exo was used to generate ssDNA from PCR amplification products. The digestion procedure was performed as the manufacturer's protocol. Reaction was carried out at 37 °C for 30 min in 1 × reaction buffer containing 0.02 U/μL of λ-Exo and 10 nmol of dsDNA with a final volume of 100 μL. The enzyme was then heat inactivated at 75 °C for 10-20 min.

3. Results and discussion

3.1. Sequence design strategy

The main purpose of our study was to distinguish between six common *EGFR* deletions. The differences between any two of the six deletion types vary in the range of 1-11 bases. Considering that only one base is different between del1 and del2, sequence design strategy was demonstrated by these two deletion types. The design strategy of target sequences was based on six common *EGFR* exon 19 deletions along with our preliminary findings to allow heterogeneous hybridization between non-complementary sequences on the electrode surface [26]. Three different DNA capture probes (CapA, CapB, and CapC) with sequences complementary to del2 were designed in order to improve biosensor specificity and optimize discrimination between del1 and del2. The difference among the three capture probes was the location of a single cytosine, which is complementary to del2 but non-complementary to del1. Relative to the mercapto (SH) end of the probe or the electrode, this cytosine was located in the distal section, the middle section, and the proximal section of CapA,

CapB, and CapC, respectively.

Subsequently, the specificity of the biosensors established based on CapA, CapB, and CapC was compared with each others. As shown in Fig. 1, the biosensors established in this study had satisfactory specificities, and allowed us to clearly distinguish a completely complementary hybridization from an incompletely complementary hybridization. Among the three capture probes, the one with the single base mismatch for del1 in the middle of its sequence (CapB) exhibited the most significant difference in current generation between del1 and del2 hybridization. In contrast, the probes with mismatches close to (CapC) or far away from (CapA) the electrode did not achieve satisfactory discrimination between del1 and del2, showing that they had less specificity than the CapB-based biosensor.

The hybridization between a capture probe and a target sequence is solid-liquid heterogeneous hybridization, in which the capture probe is fixed on a solid surface (the electrode) and thus has limited molecular motion. During such hybridization, intermolecular collisions are mainly generated by the molecular motion of target sequences, and the overall rate of inter-strand binding between DNA molecules is lower than that of liquid-phase hybridization. Nevertheless, hybridization follows similar principles under the two conditions. Temporary structural intermediates containing 2-3 base pairs are formed through intermolecular collisions, and if no additional bases are paired adjacent to the contact site, the two strands of DNA may dissociate due to molecular motion. However, if some bases are paired near the initial contact site, a more stable dsDNA intermediate may form, allowing the rest of the

complementary bases to bind together one by one like the teeth of a closing zipper to form a stable double-stranded fragment. The dissociation of a dsDNA intermediate is faster than the propagation of base-pairing when the base-pairing adjacent to the contact site is discontinuous, and thus the base pairs neighboring the intermediate's contact site play an important role in the subsequent formation of a stable double-stranded structure [27, 28]. Therefore, in hybridization reactions, the continuity (length) of a complementary sequence is of great significance to the hybridization kinetics [29]. Compared to a DNA probe where a non-complementary sequence is located near one end, the probability that an intermediate's neighboring bases do not match is greater for a DNA probe where a non-complementary sequence is located near the middle. Thus, mismatches in the middle of a DNA probe are more likely to hinder the formation of dsDNA, and reduce the efficiency of hybridization.

The location of a mismatch within a probe also affects the stability of the dsDNA structure. A dsDNA fragment with mismatches in the middle is less stable than a dsDNA fragment with mismatches at one end. This is because breaks in the middle of helical structures disrupt base-pair stacking and hydrogen bonding [30]. The less stable the dsDNA structure is, the more likely the strands will dissociate. This higher probability of dissociation further reduces the hybridization efficiency. Hence, whether the sequence in the middle section is complementary is more critical to hybridization efficiency than whether the sequence is complementary at the ends [30]. Gotoh *et al.* used an optical surface plasmon resonance biosensor to study DNA-DNA interactions. They found that the equilibrium association constants (Ka) for a

complementary hybridization and a hybridization with a single base mismatch differed maximally when the mismatch was in the middle of the DNA sequence [29]. The results of this study verify that, in a sandwich-type structure, when the non-complementary sequence is located in the middle of a capture probe, the hybridization efficiency is low and the hybridization specificity is high. Therefore, electrochemical biosensors designed to detect mismatches in the middle of their capture probes will have higher detection specificity.

Different capture probes were combined with the same reporter probe and hybridized separately with del1 and del2 targets. Relative to the electrode, CapA, CapB, and CapC have their single del1-mismatched bases at the distal end, in the middle, and at the proximal end, respectively.

3.2. Discrimination between *EGFR* deletion mutations

The six *EGFR* deletion mutants (del1-del6) were each hybridized with six different capture probes (Cd1-Cd6) and the resulting signals were compared. As shown in Fig. 2, hybridization of each target sequence with each capture probe generated a unique current signal. As expected, each probe produced the highest current when hybridized with its complementary target (i.e. Cd1 with del1, Cd2 with del2, etc.). For all other pairings, a higher degree of sequence similarity between the target sequence and the capture probe correlated with a higher current being generated by hybridization. For example, for the Cd1 probe, hybridization with del2 generated the second highest current, because del2 differs from del1 by only one base. Other target sequences that differed more strongly from del1 (del3-del6), behaved similarly and produced lower

currents than del2 when hybridized with Cd1. Likewise, for the remaining probes (Cd3-Cd6), the similarity between probe sequence and target sequence correlated well with the current generated following hybridization.

Based on the intensities of the signals and the similarities between the DNA sequences, the six deletions were divided into three groups: Group I (del1 and del2), Group II (del3 and del4), and Group III (del5 and del6). To identify which group an unknown target sequence carrying one of the six deletions belongs to, it is only necessary to hybridize it with a representative probe from each group, instead of with all six capture probes. Subsequently, further discrimination can be achieved by comparing the signals to identify the exact deletion type. Use of this method of grouping deletions based on signal similarity can reduce the workload and facilitate quick identification of the general deletion type. Any of the six common *EGFR* deletions can be roughly identified by hybridizations with three probes in one step, and precisely determined by hybridization with a fourth probe in a subsequent step.

Three deletion mutant samples (dA, dB, and dC) were used as target sequences for testing with the proposed grouping approach. First, three probes Cd2 (Group I), Cd4 (Group II), and Cd6 (Group III) were used for hybridization and the resulting currents were compared (Fig. 3). For the dA sample, the highest current value was obtained following hybridization with Cd2, whereas lower currents were obtained when it was hybridized with Cd4 or Cd6. This result suggests that dA belongs to Group I, and has either a del1 or del2 mutation. Next, the capture probe Cd1 was used for intra-group discrimination, which yielded a current of 7894.6 nA, far smaller than 10138 nA

generated by Cd2. Therefore, the dA sample was identified to be the del2 mutation. The dB sample was similarly tested using this procedure, and was found to belong to Group II in the first step, then identified as a del4 mutation in a second step. Using the same approach, the dC sample was determined to have the del5 mutation, from Group III. Therefore, by comparing the currents generated by different capture probes, *EGFR* sequences containing one of six common deletions (del1-del6) can be precisely identified. The results were all confirmed to be correct, showing that this grouped step-by-step method is effective for precise identification of the common deletion types.

3.3. Precise identification of exon 19 deletions in the *EGFR* genes of lung cancer patients

Fig. 4 shows the results of gel electrophoresis of the reverse transcription PCR (RT-PCR) amplification products of *EGFR* mRNA extracted from lung cancer patient tissues. Bright bands migrating at approximately 90 bp are seen in all lanes containing amplification products of samples from eight patients (P1-P8). Based on the results, it can be inferred the success of amplification of 90 bp high purity products, as evident from the clear single bands without tailing.

The OD_{260} and OD_{280} of the RT-PCR products from the eight patient samples were measured using a UV spectrophotometer. The ratio OD_{260}/OD_{280} was greater than 1.8 for all products. The RT-PCR product concentrations were calculated, and the samples were subsequently diluted to a concentration of approximately 10 nM by addition of

sterile water. Lastly, the products were digested with λ-Exo into single strands before electrochemical biosensor testing.

First, wild type and deletion types were distinguished. Based on our previous study, the optimal probe pair for wild-type *EGFR* detection (capture probe 5'-cggag atgtt gcttc tctta attcc-3' and reporter probe 5'-ttgat agcga cggga atttt aactt-3') was used to test the eight RT-PCR products [26]. As shown in Fig. 5, the RT-PCR products from patients P1, P2, P4, P5, P6, and P7 yielded relatively high currents of over 3000 nA, which were similar to those of the synthesized wild-type DNA by using the same DNA probe in our previous study [26]. These results inferred that these six samples were from patients who had a wild-type *EGFR* gene, which were further confirmed by sequencing. The currents observed from the P3 and P8 samples were considerably small, suggesting these two patients had deletions in their *EGFR* genes.

The P3 and P8 samples were further investigated using the grouped testing method. The Cd2, Cd4, and Cd6 probes were used in the first step screening. As shown in Figure 6, the P3 sample generated the highest current when hybridized with the Cd2 probe, suggesting that it belongs to Group I (del1 or del2). The strongest signal was observed from the P8 sample after hybridization with Cd6, indicating that P8 likely belongs to Group III (del5 or del6).

After P3 was classified as being in Group I, and P8 as being Group III, the next step was to identify their exact deletion types. The Cd1 capture probe from Group I and the Cd5 from Group III were used for intra-group discrimination. As shown in Fig. 6, the current generated by the P3 sample hybridizing with the Cd1 probe was smaller

than the current generated by the P3 sample hybridizing with the Cd2 probe. This suggests that patient P3 has an *EGFR* gene with a del2 type mutation. The current generated by combining the P8 sample with the Cd5 probe was greater than that generated by combining it with the Cd6 probe, suggesting that patient P8 has an *EGFR* gene with a del5 type mutation. The above results were all consistent with subsequently obtained sequencing results (Fig. 7), proving that this approach is capable of distinguishing deletion types.

4. Conclusions

The main objectives of this study were to improve electrochemical biosensor specificity, and to effectively distinguish between six common deletion variants of *EGFR* exon 19 using these sensors. Based on preliminary studies, we investigated the influence of the location of a non-complementary sequence within a DNA capture probe on the hybridization specificity. Different probes were tested in a heterogeneous hybridization environment on the surface of an electrode. The results revealed that a probe with the non-complementary sequence located in its middle part has the highest hybridization specificity, and can even differentiate between two sequences that differ by only one base. Based on this finding, capture probes were designed to detect six common deletions within exon 19 of the *EGFR* gene. Further, based on the observed patterns of signal intensities, a grouping approach was proposed to reduce the workload, simplify the operation, and realize faster identification of specific mutations. The grouping method was used to analyze the RT-PCR products from lung cancer patients. The identification results were consistent with sequencing results,

confirming the applicability of the proposed method.

Acknowledgment

The authors gratefully acknowledge the financial support of the National High Technology and Development of China (863 Project, 2012AA022604), the National Natural Science Foundation of China (21675024), the Natural Science Foundation of Fujian Province (2015J01415, 2016J01426), and Program for Innovative Leading Talents in Fujian Province (2016B016).

Reference

[1] J.H. Schiller, D. Harrington, C.P. Belani, C. Langer, A. Sandler, J. Krook, J. Zhu, D.H. Johnson, Comparison of four chemotherapy regimens for advanced non–small-cell lung cancer, New Engl. J. Med. 346 (2002) 92-98.

[2] M. Fukuoka, S. Yano, G. Giaccone, T. Tamura, K. Nakagawa, J.Y. Douillard, Y. Nishiwaki, J. Vansteenkiste, S. Kudoh, D. Rischin, R. Eek, T. Horai, K. Noda, I. Takata, E. Smit, S. Averbuch, A. Macleod, A. Feyereislova, R.P. Dong, J. Baselga, Multi-institutional randomized phase II trial of gefitinib for previously treated patients with advanced non-small-cell lung cancer, J. Clin. Oncol. 21 (2003) 2237-2246.

[3] X.W. Zhang, J. Gureasko, K. Shen, P.A. Cole, J. Kuriyan, An allosteric mechanism for activation of the kinase domain of epidermal growth factor receptor, Cell 125 (2006) 1137-1149.

[4] R. Bose, X.W. Zhang, The ErbB kinase domain: Structural perspectives into

kinase activation and inhibition, Exp. Cell Res. 315 (2009) 649-658.

[5] C.H. Yun, T.J. Boggon, Y.Q. Li, M.S. Woo, H. Greulich, M. Meyerson, M.J. Eck, Structures of lung cancer-derived EGFR mutants and inhibitor complexes: Mechanism of activation and insights into differential inhibitor sensitivity, Cancer Cell 11 (2007) 217-227.

[6] A. Kumar, E.T. Petri, B. Halmos, T.J. Boggon, Structure and clinical relevance of the epidermal growth factor receptor in human cancer, J. Clin. Oncol. 26 (2008) 1742-1751.

[7] J.Y. Douillard, F.A. Shepherd, V. Hirsh, T. Mok, M.A. Socinski, R. Gervais, M.L. Liao, H. Bischoff, M. Reck, M.V. Sellers, Molecular predictors of outcome with gefitinib and docetaxel in previously treated non–small-cell lung cancer: data from the randomized phase III INTEREST trial, J. Clin. Oncol. 28 (2010) 744-752.

[8] T.S. Mok, Y.S. Wu, Gefitinib or carboplatin-paclitaxel in pulmonary adenocarcinoma, New Engl. J. Med. 361 (2009) 947-957.

[9] J. Zhang, S. Song, L. Wang, D. Pan, C. Fan, A gold nanoparticle-based chronocoulometric DNA sensor for amplified detection of DNA, Nat. Protoc. 2 (2007) 2888-2895.

[10] W. Chen, Y.H. Liu, H.N. Li, A.L. Liu, X.H. Lin, Y.Z. Chen, Ultrasensitive and facile electrochemical deoxyribonucleic acid biosensor based on the conformational change of the recognition interface, Anal. Chim. Acta 748 (2012) 89-94.

[11] B. Kannan, D.E. Williams, M.A. Booth, J. Travas-Sejdic, High-sensitivity, label-free DNA sensors using electrochemically active conducting polymers, Anal.

Chem. 83 (2011) 3415-3421.

[12] L.Q. Lin, Q.C. Liu, L.M. Wang, A.L. Liu, S.H. Weng, Y. Lei, W. Chen, X.H. Lin, Y.Z. Chen, Enzyme-amplified electrochemical biosensor for detection of PML-RAR alpha fusion gene based on hairpin LNA probe, Biosens. Bioelectron. 28 (2011) 277-283.

[13] E. Dubuisson, Z.Y. Yang, K.P. Loh, Optimizing Label-free DNA electrical detection on graphene platform, Anal. Chem. 83 (2011) 2452-2460.

[14] J. Zhang, S.P. Song, L.Y. Zhang, L.H. Wang, H.P. Wu, D. Pan, C.H. Fan, Sequence-specific detection of femtomolar DNA via a chronocoulometric DNA sensor (CDS): Effects of nanoparticle-mediated amplification and nanoscale control of DNA assembly at electrodes, J. Am. Chem. Soc. 128 (2006) 8575-8580.

[15] J. Wu, S. Campuzano, C. Halford, D.A. Haake, J. Wang, Ternary surface monolayers for ultrasensitive (zeptomole) amperometric detection of nucleic acid hybridization without signal amplification, Anal. Chem. 82 (2010) 8830-8837.

[16] A. Bonanni, M. Pumera, Graphene platform for hairpin-DNA-based impedimetric genosensing, ACS Nano 5 (2011) 2356-2361.

[17] F. Xia, R.J. White, X. Zuo, A. Patterson, Y. Xiao, D. Kang, X. Gong, K.W. Plaxco, A.J. Heeger, An electrochemical supersandwich assay for sensitive and selective DNA detection in complex matrices, J. Am. Chem. Soc. 132 (2010) 14346-14348.

[18] G. Liu, Y. Wan, V. Gau, J. Zhang, L.H. Wang, S.P. Song, C.H. Fan, An enzyme-based E-DNA sensor for sequence-specific detection of femtomolar DNA

targets, J. Am. Chem. Soc. 130 (2008) 6820-6825.

[19] Y.Q. Ren, H.M. Deng, W. Shen, Z.Q. Gao, A highly sensitive and selective electrochemical biosensor for direct detection of microRNAs in serum, Anal. Chem. 85 (2013) 4784-4789.

[20] K. Wang, Y. Lei, G.X. Zhong, Y.J. Zheng, Z.L. Sun, H.P. Peng, W. Chen, A.L. Liu, Y.Z. Chen, X.H. Lin, Dual-probe electrochemical DNA biosensor based on the "Y" junction structure and restriction endonuclease assisted cyclic enzymatic amplification for detection of double-strand DNA of PML/RAR alpha related fusion gene, Biosens. Bioelectron. 71 (2015) 463-469.

[21] H. Gao, X. Jiang, Y.J. Dong, W.X. Tang, C. Hou, N.N. Zhu, Dendrimer-encapsulated copper as a novel oligonucleotides label for sensitive electrochemical stripping detection of DNA hybridization, Biosens. Bioelectron. 48 (2013) 210-215.

[22] I. Grabowska, D.G. Singleton, A. Stachyra, A. Gora-Sochacka, A. Sirko, W. Zagorski-Ostoja, H. Radecka, E. Stulz, J. Radecki, A highly sensitive electrochemical genosensor based on Co-porphyrin-labelled DNA, Chem. Commun. 50 (2014) 4196-4199.

[23] H. Gao, X. Jiang, Y.J. Dong, W.X. Tang, C. Hou, N.N. Zhu, Dendrimer-encapsulated copper as a novel oligonucleotides label for sensitive electrochemical stripping detection of DNA hybridization, Biosens. Bioelectron. 48 (2013) 210-215.

[24] M.Ç. Canbaz, C.S. Simşek, M.K. Sezgintürk, Electrochemical biosensor based

on self-assembled monolayers modified with gold nanoparticles for detection of HER-3, Anal. Chim. Acta 814 (2014) 31-38.

[25] C.J. Yu, Y. Wan, H. Yowanto, J. Li, C. Tao, M.D. James, C.L. Tan, G.F. Blackburn, T.J. Meade, Electronic detection of single-base mismatches in DNA with ferrocene-modified probes, J. Am. Chem. Soc. 123 (2001) 11155-11161.

[26] X.W. Xu, X.H. Weng, C.L. Wang, W.W. Lin, A.L. Liu, W. Chen, X.H. Lin, Detection EGFR exon 19 status of lung cancer patients by DNA electrochemical biosensor, Biosens. Bioelectron. 80 (2016) 411-417.

[27] D. Pörschke, M. Eigen, Co-operative non-enzymic base recognition. 3. Kinetics of the helix-coil transition of the oligoribouridylic-oligoriboadenylic acid system and of oligoriboadenylic acid alone at acidic pH, J. Mol. Biol. 62 (1971) 361-381.

[28] M.E. Craig, D.M. Crothers, P. Doty, Relaxation kinetics of dimer formation by self complementary oligonucleotides, J. Mol. Biol. 62 (1971) 383-392.

[29] M. Gotoh, Y. Hasegawa, Y. Shinohara, M. Schimizu, M. Tosu, A new approach to determine the effect of mismatches on kinetic parameters in DNA hybridization using an optical biosensor, DNA Res. 2 (1995) 285-293.

[30] S.L.J. Jr, D. Hicks, The thermodynamics of DNA structural motifs, Annu. Rev. Biophys. Biomol. Struct. 33 (2004) 415-440.

[31] Y.H. Liu, H.N. Li, W. Chen, A.L. Liu, X.H. Lin, Y.Z. Chen, Bovine serum albumin-based probe carrier platform for electrochemical DNA biosensing, Anal. Chem. 85 (2013) 273-277.

Figures

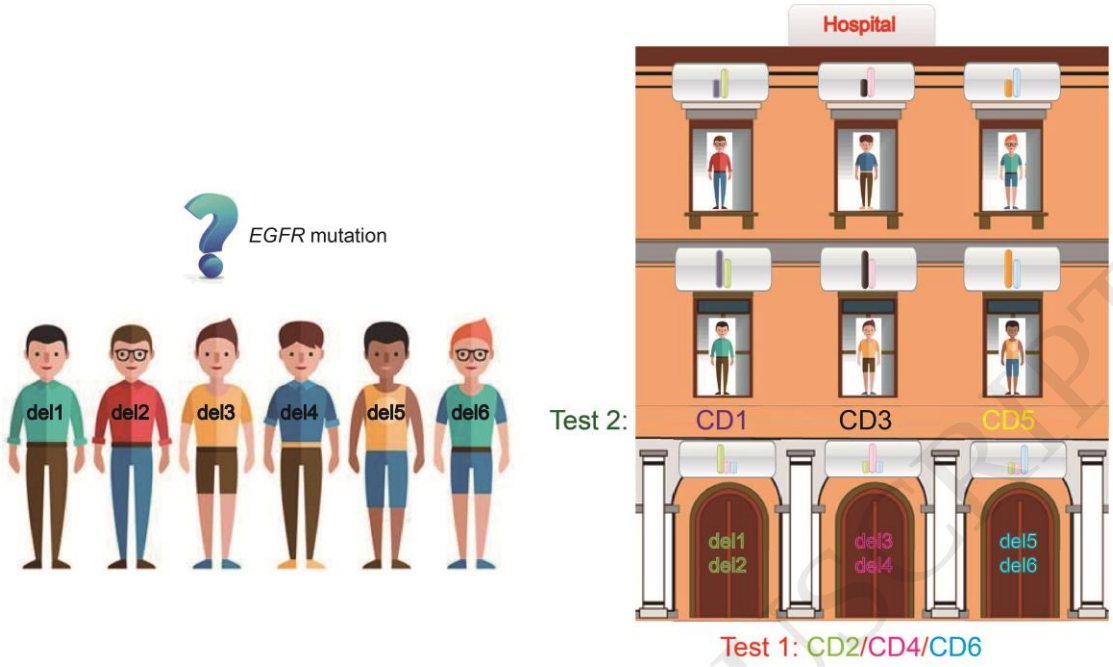

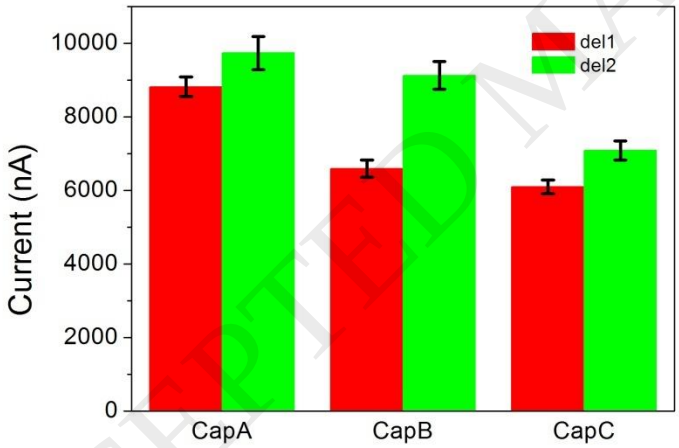

Fig. 1. Influence of non-complementary base location on biosensor specificity.

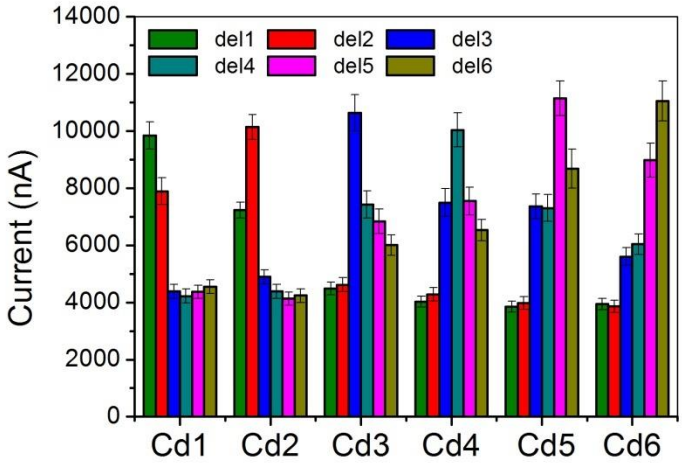

Fig. 2. Analysis of the hybridization of deletion mutants with different capture probes. The graph shows currents measured after hybridizations between the six *EGFR* deletion mutants (del1-del6) and six different capture probes (Cd1-Cd6).

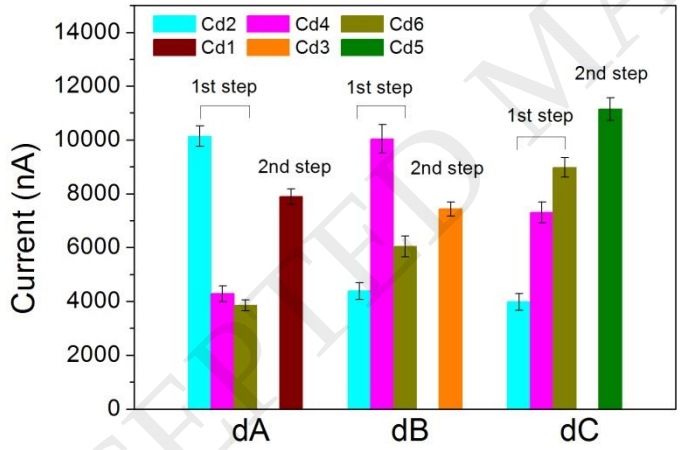

Fig. 3. Identification of mutation types using a grouped-testing approach.

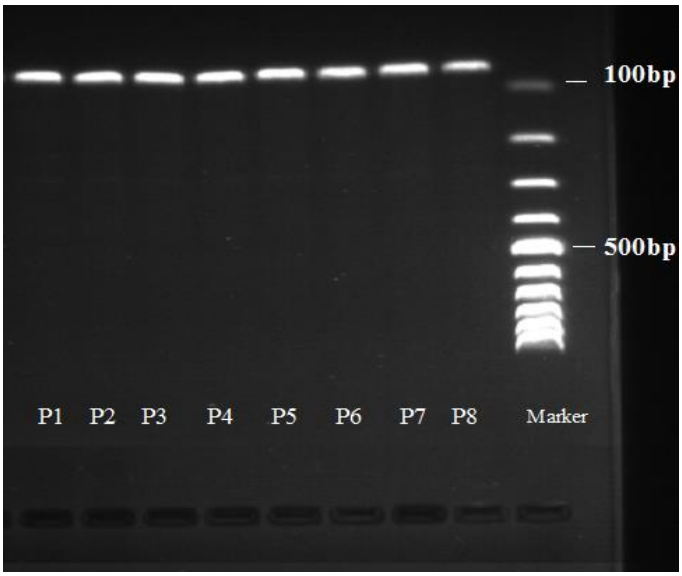

Fig. 4. Analysis of the RT-PCR amplicons by gel electrophoresis in a 1.5 % agarose gel containing 0.5 μg/mL ethidium bromide. Lanes 1-8: PCR products of patients P1-P8. Lane 9: marker.

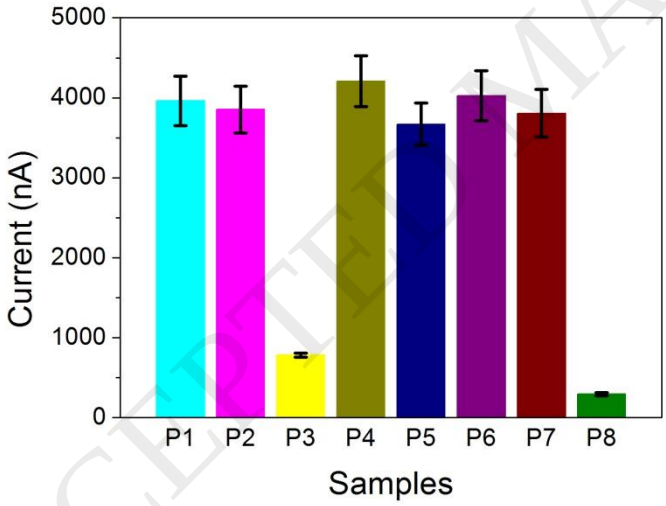

Fig. 5. Current generated by the digested RT-PCR products of *EGFR* mRNA from eight patient samples using probe pair for wild-type *EGFR*.

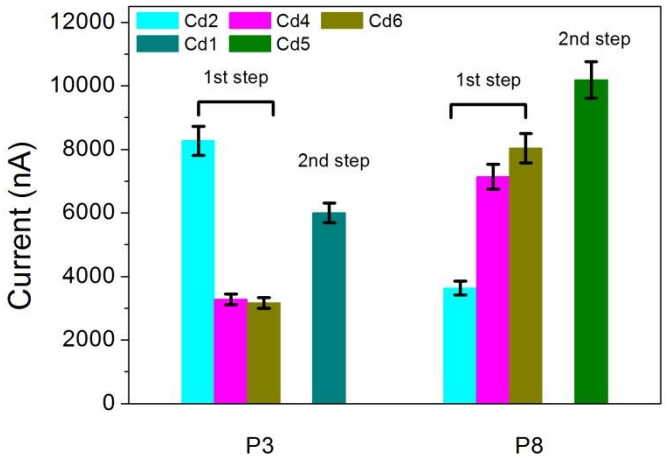

Fig. 6. Mutation type identification of real samples using the grouped testing method.

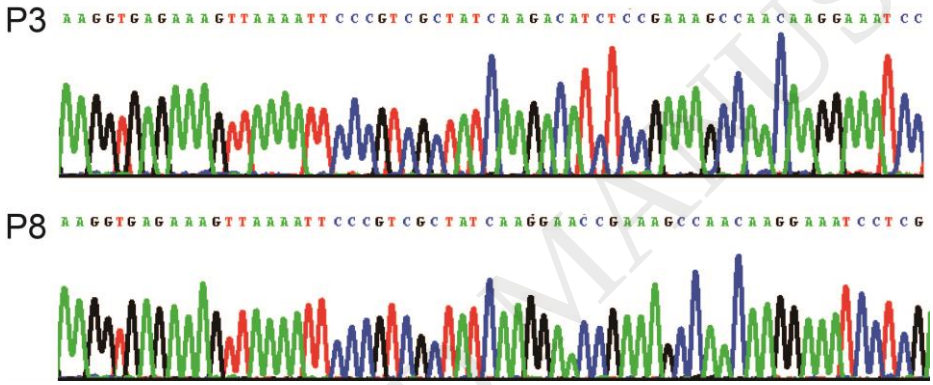

Fig. 7. Chromatograms showing partial sequencing results from the RT-PCR products from actual patient samples P3 and P8.